



**HAL**  
open science

## Modelling of the ultrasonic propagation in polycrystalline materials

Lili Ganjehi, Vincent Dorval, Frederic Jenson

► **To cite this version:**

Lili Ganjehi, Vincent Dorval, Frederic Jenson. Modelling of the ultrasonic propagation in polycrystalline materials. Acoustics 2012, Apr 2012, Nantes, France. hal-00810720

**HAL Id: hal-00810720**

**<https://hal.science/hal-00810720>**

Submitted on 23 Apr 2012

**HAL** is a multi-disciplinary open access archive for the deposit and dissemination of scientific research documents, whether they are published or not. The documents may come from teaching and research institutions in France or abroad, or from public or private research centers.

L'archive ouverte pluridisciplinaire **HAL**, est destinée au dépôt et à la diffusion de documents scientifiques de niveau recherche, publiés ou non, émanant des établissements d'enseignement et de recherche français ou étrangers, des laboratoires publics ou privés.



# ACOUSTICS 2012

## Modelling of the ultrasonic propagation in polycrystalline materials

L. Ganjehi, V. Dorval and F. Jenson

Commissariat à l'énergie atomique, Centre de Saclay - PC120, 91191 Gif-Sur-Yvette, France  
lili.ganjehi@cea.fr

In some polycrystalline materials, ultrasonic non destructive testing is affected by structural noise and attenuation. Those phenomena can cause significant loss in detection performances. Thus, the presence of a microstructure is a limiting factor of ultrasonic inspection capabilities and it must be accounted for when designing new NDE methods. Modeling work has been underway at CEA-LIST in the software CIVA to describe attenuation, structural noise and distortions appearing when a wave propagates in a heterogeneous medium such as a polycrystalline material. The objective is to develop new simulation tools based on metallurgical data input. To achieve this goal, a theoretical model relating ultrasonic scattering to properties of the microstructure and its integration to existing algorithms, allowing us to compute structural noise and attenuation from material properties is proposed. Further numerical study and comparisons with experimental results have been performed to study the influence of the type of structure (monophasic or biphasic), the shape (equiaxed or elongated) and the size of grains.

## 1 Introduction

Some rotating engine components are manufactured in titanium alloy or nickel alloy, material which has a two-phase microstructure governed by several length scales. In ultrasonic inspections of aircraft engine components, the detectability of critical defects can be limited by grain noise. This is the case for subtle defects, such as hard- $\alpha$  inclusion in titanium alloys, where the difference between the acoustic impedances of the defect and host material is small. A quantitative description of grain noise and attenuation in such alloys is essential to estimate accurately flaw detection reliability.

A model for the propagation of ultrasonic waves in a polycrystalline material as a function of the morphologic and elastic properties has been implemented in the non-destructive testing software, CIVA ([1], CEA-LIST). The objective is to verify that the modeling developments are able to take into account the physical phenomena induced by the complexity of material constituting the inspected aeronautical metallic parts. Our study focuses on the coexistence of two phases as a cause of the noise level. The comparison between experimental and numerical results of noise level shows a good agreement in the sample described by a biphasic and elongated structure such as titanium alloy.

## 2 Description of the two-phases structure

The titanium alloy is composed of two phases  $\beta$  and  $\alpha$  [2]. During the solidification of the metal, the  $\beta$  phase appears first and forms macrograins. A macrograin is defined as a zone in which the  $\beta$  phase has a given crystallographic orientation. The orientation of a macrograin is assumed to be random. The  $\alpha$  phase appears later in groups of needle-shaped crystals called crystallites. A group of crystallites having the same crystallographic orientation is called a colony. Such structures can be seen in Figure 1.

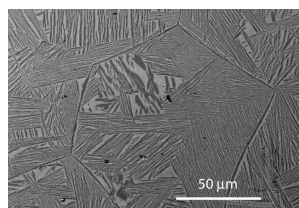


Figure 1: Micrograph of a two-phase titanium alloy microstructure [2].

The microstructure of the studied sample is close to the example of the Figure 1. In order to develop the model, we assume that the crystallites are too small to induce scattering. Therefore, macrograins and colonies are the only heterogeneities taken into account in the computation of the scattering. The modelled two-scale structure is represented in the Figure 2. The description of the microstructure can be summarized as follow: each macrograin contains a first phase of random orientation. It is separated in several colonies which contain the second phase of a given orientation. The orientation of the second phase of a colony is dependent on the orientation of the first phase of the macrograin [3].

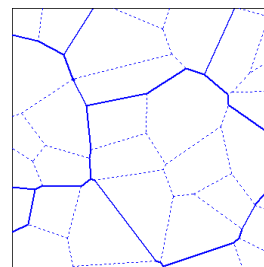


Figure 2: Model of the two-phases microstructure (full lines are boundaries between macrograins, dotted lines are boundaries between colonies).

## 3 Description of the analytical model

### 3.1 Scattering coefficient

The effect of the microstructure of the polycrystalline specimen on the ultrasonic propagation is defined by the backscattering coefficient  $\eta$ . The backscattering coefficient depends on the morphological and elastic properties of the specimen, the wavelength and the type of the transmitted wave. An analytical model based on the approach proposed by Gubernatis *et al.* [4] and Margetan *et al.* [5] was developed. A random, isotropic and statistical homogeneous set of scatterers characterized by a variation of elastic properties is considered:

$$\Delta C_{ijkl}(\vec{r}) = C_{ijkl}(\vec{r}) - C_0$$

$$\text{with } C_0 = \langle C_{ijkl} \rangle$$

The analytical model is based on the Born approximation (weak scattering) and the multiple scattering is neglected. For the case of single-phase materials, backscattering is caused by acoustic impedance fluctuations which are directly related to the orientation of grains. For

the two-phases case, the backscattering is caused not only by the acoustic impedance fluctuation of each phase (controlled by the grain orientation) but also by the contrast between phases. This effect may be considered negligible if signals backscattered from phase boundaries are dominant and no orientation relationship is present between phases. In the titanium alloy case, the backscattered noise signals may be strongly influenced by crystallographic orientation relationships between phases. Based on some additional assumptions: i) random orientation of prior grains is assumed, ii) each variant occurs with equal probability and iii) individual crystallites are too small to make a significant contribution to the grain noise, the result for the backscattered coefficient ( $\theta = \pi$ ) for a longitudinal wave propagating is given by:

$$\eta^{L \rightarrow L} = \frac{k_i^4}{(4\pi\rho V_l)^2} [\langle \Delta C_{3333}^M \Delta C_{3333}^M \rangle f + \langle \Delta C_{3333}^C \Delta C_{3333}^C \rangle g]$$

$$\text{with } f = \int d\vec{s} W^M(\vec{s}) \exp(2ik_i s)$$

$$\text{and } g = \int d\vec{s} W^M(\vec{s}) W^C(\vec{s}) \exp(2ik_i s)$$

where  $\rho$  is the density and  $V_l$  is the longitudinal wave velocity. The indices  $M$  and  $C$  design respectively the macrograins and the colonies. The backscatter coefficient is related to the morphological and elastic properties of the macrograins and colonies of the scattering medium by two functions:

- $W(\vec{s})$  is the probability that two points  $\vec{r}$  and  $\vec{r}'$  ( $|\vec{s}| = |\vec{r} - \vec{r}'|$ ) would fall within the same grain, a condition that causes their elastic constants to be identical. The functional form of  $W(\vec{s})$  is controlled by the distribution of grain sizes.
- The quantity  $\langle \Delta C_{3333}^M \Delta C_{3333}^M \rangle$  is an ensemble average of the product of the variant elastic moduli, averaged over all macrograins (designed by  $M$ ) and colonies (designed by  $C$ ) orientations. The ensemble average elastic constant product terms will be obtained by considering the orientations relationship between the sample, the macrograins and the colonies.

An exponential form is assumed for both  $W_M$  and  $W_C$

$$W_M(\vec{x}, \vec{x}') = \exp\left[-\frac{|\vec{x}' - \vec{x}|}{a_{Macro}}\right]$$

$$W_C(\vec{x}, \vec{x}') = \exp\left[-\frac{|\vec{x}' - \vec{x}|}{a_{colo}}\right]$$

Such forms are often used for correlation functions in polycrystalline materials. The lengths  $a_{Macro}$  and  $a_{colo}$  are referred to as an effective radius grain size, respectively for macrograins and colonies. These expressions assume that grains are equiaxed. This model has been recently extended to the elongated shape cases. Furthermore, [5] gives the result for a transversal wave.

Examples of plots of the backscattering coefficients for both longitudinal and transverse waves are presented in Figure 3. They are compared to plots of backscattering coefficients obtained assuming that the material is entirely made of  $\beta$  phase grains of the size of macrograins or of  $\alpha$  phase grains of the size of colonies.

As in the single phase case, higher scattering coefficients are obtained for transverse waves than for longitudinal waves. In both cases, the backscattering coefficient for two-phases case has a frequency dependency similar to the macrograin coefficient for low frequencies and to the colonies coefficient for the higher frequencies. It confirms that is necessary to take into account both scales of the material structure in order to be able to properly model the scattering at all frequencies.

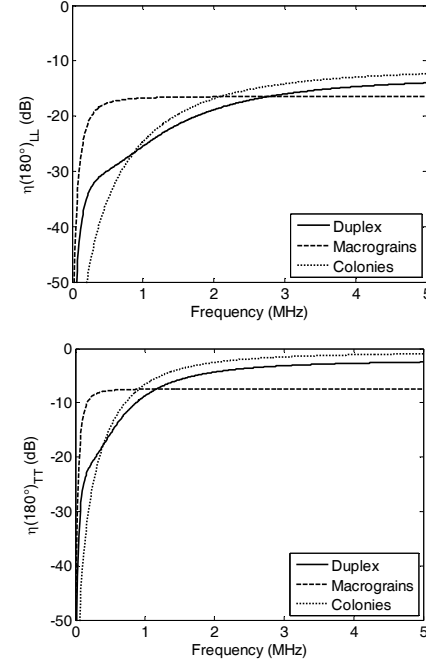


Figure 3: Backscattering coefficients obtained assuming the following material properties:  $\rho=4500 \text{ kg/m}^3$ ,  $v_L=6072 \text{ m/s}$ ,  $v_T=3127 \text{ m/s}$ ,  $p_\alpha=80\%$ ,  $a_{Macro}=2.5\text{mm}$ ,  $a_{colo}=0.25\text{mm}$ ,  $C_{11}^\alpha=162.4 \text{ GPa}$ ,  $C_{12}^\alpha=92 \text{ GPa}$ ,  $C_{13}^\alpha=69 \text{ GPa}$ ,  $C_{44}^\alpha=46.7 \text{ GPa}$ ,  $C_{11}^\beta=134 \text{ GPa}$ ,  $C_{12}^\beta=110 \text{ GPa}$ ,  $C_{44}^\beta=36 \text{ GPa}$ . The reference for dBs is arbitrary.

### 3.2 Attenuation coefficient

The material attenuation coefficient depends on the relative grain size with respect to the wavelength. Let us denote the wavelength  $\lambda$ , the frequency by  $f$ , the average diameter of a material grain  $D$  and some constants by  $c_1$ ,  $c_2$ ,  $c_3$ . Then, in the Rayleigh region ( $\lambda \gg D$ ), we have  $\alpha(f) = c_1 D^3 f^4$ , in the stochastic region ( $\lambda \sim D$ ), we have  $\alpha(f) = c_2 D f^2$  and in the diffusion regime ( $\lambda \ll D$ ), we have  $\alpha(f) = c_3 D f$ .

Attenuation coefficients can be expressed as a function of the scattering coefficient, using the same relationships as used by Dorval *et al.* [6] in the case of single phase materials:

$$\alpha_L = \pi \int_{\theta=0}^{\pi} \sin(\theta) [\eta_{L \rightarrow L}(\theta) + \eta_{L \rightarrow TH}(\theta) + \eta_{L \rightarrow TV}(\theta)] d\theta$$

$$\alpha_T = \frac{\pi}{2} \int_{\theta=0}^{\pi} \sin(\theta) \left[ \begin{array}{l} \eta_{TH \rightarrow L}(\theta) + \eta_{TH \rightarrow TH}(\theta) \\ + \eta_{TH \rightarrow TV}(\theta) + \eta_{TV \rightarrow L}(\theta) \\ + \eta_{TV \rightarrow TH}(\theta) + \eta_{TV \rightarrow TV}(\theta) \end{array} \right] d\theta$$

$\theta$  is the scattering angle and TH and TV indicate transverse waves polarized respectively in horizontal and vertical directions. These expressions are obtained based on the assumption that the attenuation coefficients correspond

to a decay of the wave energy entirely due to a loss of energy by scattering.

For both L and T waves, the attenuation coefficient for the two-phases structure (Fig. 4) is between the attenuations for macrograins and for colonies. For the case of L waves it is very close to the attenuation due to colonies, but this is not a general behavior, as it is strongly dependent on the properties of the material.

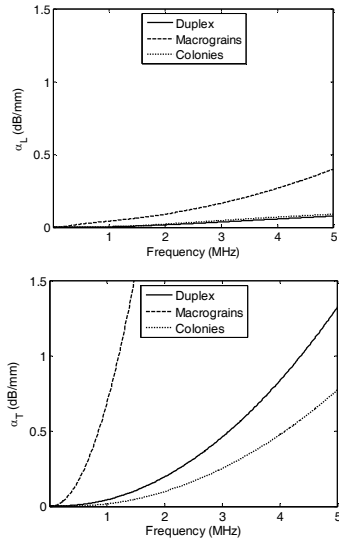


Figure 4: Attenuation coefficients obtained using the same properties as in Figure 3.

## 4 Experimental results

The goal of this section is to quantify experimentally the mean noise level as a function of time taking into account the two correlated phenomena: structural noise and attenuation. The experimental data will allow to evaluate both the accuracy of the representation of the microstructure and the validity of the approximations of the methods (Born and single scattering).

### 4.1 Experimental setup

Ultrasonic measurements were performed in immersion at normal incidence using a focused transducer provided by Snecma (Safran group). The main characteristics of the transducer are a focal length  $F$  of 406.2 mm, a diameter of 25.4 mm and a center frequency  $f_0$  of 10 MHz.

Pulse/echo acquisitions were performed on a cubic specimen in titanium alloy with a depth of 70mm. Longitudinal-wave properties which include attenuation and backscattered noise parameters were measured. Three measurements corresponding to three different entry faces have been carried out (Fig.5).

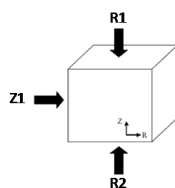


Figure 5: Geometry of the sample.

Figure 6 shows the pulse/echo acquisition for backscattered noise measurement. The waterpath  $z_M$  was chosen such that the beam was focused in the half depth of the block. The reference for measurement is the amplitude of the echo coming from the flat bottom hole of the reference part.

The transducer is scanned in a rectangular grid (10mm\*10mm with a step of 0.1mm) above the specimen to acquire noise echoes. At each transducer position, the temporal (Ascan) noise signal is digitized and averaged to decrease the impact of the electronic noise (electronic noise will always be present at some level and, hence, contribute to the measured noise)

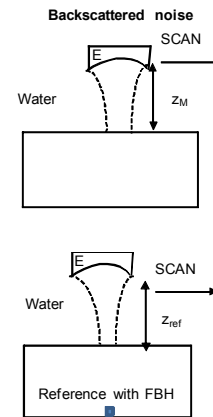


Figure 6: Pulse/echo acquisition for backscattered noise measurement.

### 4.2 Mean noise level as a function of time

One example of the backscattered noise measurement is illustrated in Figure 7. The spatial representation (Fig.7, left part) shows the gated-peak-to-peak backscattered grain noise seen through face R1 of the cubic specimen.

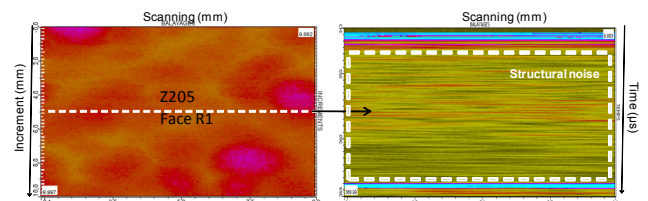


Figure 7: Spatial representation (Cscan, left part) and spatio-temporal representation (Bscan, right part) of backscattered signals measured for the face R1 of the cubic specimen.

Figure 8 shows the mean noise level as a function of time  $M(t)$  measured for the R1 face of the cubic specimen as discrete data points with the errors bars indicating  $\pm$  one standard deviation.  $M(t)$  is obtained by averaging the Hilbert Transform of Ascans over the measurement window depths (dashed line in Fig. 7, right).  $M(t)$  is normalized by the amplitude of the reference signal. The black line indicates the electronic noise level.

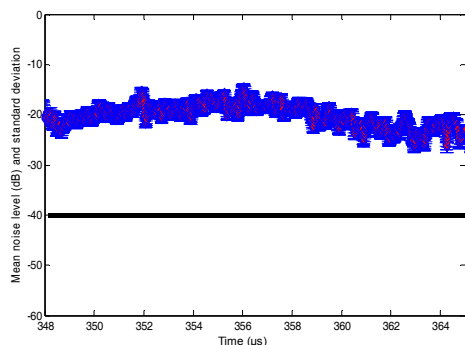


Figure 8: The average values of backscattered noise function. The discrete data points (red) are the experimental estimates and the error bar (blue) indicate +/- one standard deviation. The solid curve is the electronic noise level

## 5 Numerical results: Influence of the two-phase elongated

The scattering and attenuation coefficients obtained with the model are used by a computational method implemented in the CIVA software (available at the end of 2012). This method is identical to the one described by Dorval *et al.* [6] for the case of single phase materials: only the scattering and attenuation coefficients have to be modified according to the structure.

The general principles of the noise scattering method are outlined in Figure 9.

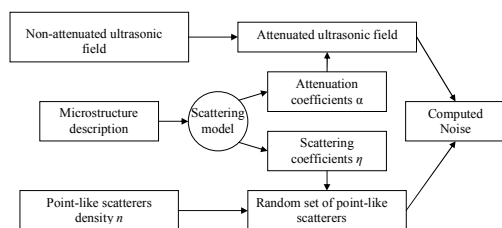


Figure 9: Principle of the noise scattering method.

Simulations were performed on the cubic specimen of 70mm depth along X axis with the focused transducer (Fig.10). Three kinds of simulations have been realized. First, the metallurgical structure of the sample is characterized by a monophasic structure and composed of equiaxed macrograins. We will show that this description is not sufficient to determine the mean noise level in the specimen. Secondly, the structure of the sample is characterized by a biphasic structure. It is composed by equiaxed macrograins and equiaxed colonies. Several simulations show that the noise level is better predicted taking into account the influence of colony. Finally, the agreement between experimental and numerical results is very good taking into account elongated and biphasic metallurgical structure.



Figure 10: Backscattered noise simulation in the cubic specimen.

### 5.1.1 Monophasic equiaxed structure

First, we consider a monophasic equiaxed structure. The input parameters are listed just below.

Input parameters	Source
Elastic constants	Bibliographic study
Type of symmetry	Bibliographic study
Macrograin size	Metallurgical study

Table 1: Input parameters of noise generator and source of data in a single-phase equiaxed structure.

A parametric study shows that the maximum of noise level is obtained with a size of macrograin  $a_{macro} = 100 \mu m$ . Figure 11 shows the comparison of the mean noise level as a function of time simulated in monophasic equiaxed structure with  $a_{macro} = 100 \mu m$  (Fig. 11, black) with the experimental result acquired in the cubic specimen on R1 face (Fig.11, blue). The mean noise level as a function of time is much smaller than those obtained experimentally.

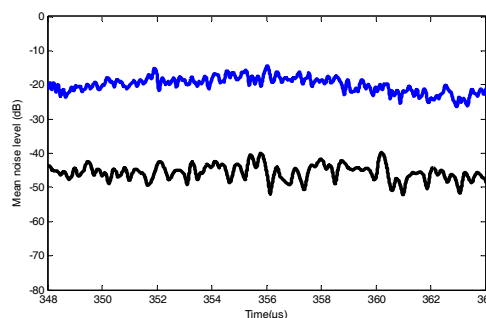


Figure 11: Mean noise level of the backscattered noise in a monophasic equiaxed structure at 10MHz with  $a_{macro}=100\mu m$  (black) and experimental results in the cubic specimen (face R1, blue).

### 5.1.2 Biphasic equiaxed structure

Secondly, we consider a two-phase equiaxed structure. The input parameters are listed in Table 2:.

Input parameters	Source
Elastic constants	Bibliographic study
Type of symmetry	Bibliographic study
Macrograin mean size	Metallurgical study
Colony mean size	Parametric + metall. study
Pourcentage of each phase	Metallurgical study

Table 2: Input parameters of noise generator and source of data in a two-phase equiaxed structure.

Taking into account the colonies, Figure 12 shows the comparison of the mean noise level between experimental results and CIVA results with equiaxed macrograins,  $a_{macro} = 100 \mu m$  and  $a_{colo} = 12.5 \mu m$ . The agreement of the mean noise level as a function of time is much better than the previous description of the monophasic structure. Taking into account the biphasic structure improves the noise level. But, this result could be improved taking into account the elongated shape of macrograins

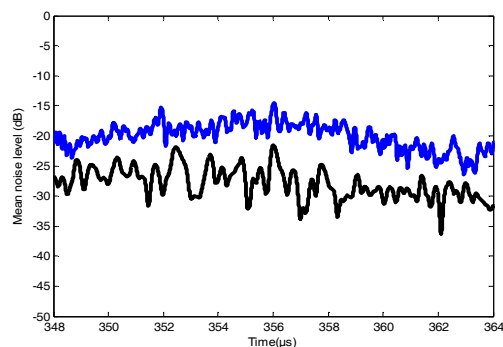


Figure 12: Comparison between measured mean noise level at 10 MHz (blue) face R1 and simulated noise (black) with equiaxed macrograins  $a_{\text{macro}}=100\mu\text{m}$  and  $a_{\text{colo}} = 12.5\mu\text{m}$ .

### 5.1.3 Biphasic elongated structure

Finally, we consider a two-phases elongated structure which is coherent with the metallurgical structure provided by Snecma (Safran group).

Input parameters	Source
Elastic constants	Bibliographic study
Type of symmetry	Bibliographic study
Macrograin mean size	Metallurgical study
Colony mean size	Parametric + metall. study
Percentage of each phase	Metallurgical study
Morphological texture	Metallurgical study

Table 3: Input parameters of noise generator and source of data in a two-phase elongated structure.

Figure 13 shows the comparison of the mean noise level between experimental result and CIVA result with elongated (ellipsoidal shape) macrograins perpendicular to the incident propagation and  $a_{\text{macro}} = 100\mu\text{m}$  and  $a_{\text{colo}} = 12.5\mu\text{m}$ . This description is coherent with the metallurgical structure. It improves the comparison between experimental and numerical results. Therefore, the improvement of the predictability of the mean noise level depends on the knowledge of the shape of macrograins and the characteristics of biphasic structure (colony size and percentage of each phase).

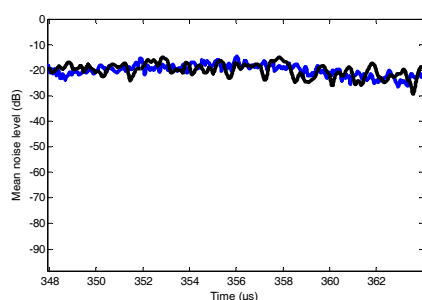


Figure 13: Comparison between measured mean noise level at 10 MHz (blue) face R1 and simulated noise (black) with elongated macrograins  $a_{\text{macro}}=100\mu\text{m}$  and  $a_{\text{colo}} = 12.5\mu\text{m}$ .

## 5 Conclusion

This work deals with the modelling of the ultrasonic inspection of aeronautical metallic part. In this scope, the CEA-LIST developed a specific model simulating the

propagation of ultrasonic waves in two-phase titanium alloy. This model uses an existing approach to account for the scattering of ultrasonic waves in polycrystals. This approach assumes that the scattering is due to the difference in elastic properties from one grain to another and relies on the Born approximation. This document presents here a general approach valid for any mode and direction. The coefficients given by this model are intended to be used by a computational method previously developed at the CEA.

The good agreement of mean noise level as a function of time between the experimental and CIVA results show the influence of the morphologic texture of the medium and the influence of the colonies (size of colony and percentage of each phase). Other comparisons have been performed in titanium alloy with biphasic equiaxed structure or in steel alloy with different size, shape and elastic constants of grains. The comparisons show a good agreement between experimental and numerical results. Our results are coherent with the results obtained recently by Lobkis *et al.*[7] on titanium alloy.

## Acknowledgements

The work leading to this publication has received funding from the European Commission Seventh Framework Programme (FP7/2007-2013) under grant agreement n° 234117 : PICASSO project.

The conditions of experimental setup and the metallurgical study have been provided by Snecma (Safran group) NDT department of Villaroche and Metallurgical department of Genevilliers and Corbeil.

## References

- [1] [www-civa.cea.fr/](http://www-civa.cea.fr/)
- [2] J. Da Costa Teixeira *et al.*, "Modeling of the effect of the  $\beta$  phase deformation on the  $\alpha$  phase precipitation in near  $\beta$ -titanium alloys", *Acta Mater* 54, 4261-4271 (2006).
- [3] Y.Han and R.B.Thompson, "Ultrasonic backscattering in duplex microstructures: Theory and application to titanium alloys", *Metall. Mater. Trans. A* 28 (1), 91-104 (1997).
- [4] J.E. Gubernatis *et al.*, "Formal aspects of the theory of the scattering of ultrasound by flaws in elastic materials", *Journal of Applied Physics* 48 (7), 2804-2811 (1977).
- [5] F.J. Margetan *et al.*, "Computation of grain-noise scattering coefficients for ultrasonic pitch/catch inspections of metals", *Rev.Prog.QNDE* 24, 1300-1307 (2005).
- [6] V. Dorval *et al.*, "Accounting for structural noise and attenuation in the modeling of ultrasonic testing of polycrystalline materials", *Rev. Prog. QNDE* 29, 1309-1316 (2010).
- [7] O.I. Lobkis *et al.*, "Ultrasonic backscattering in polycrystals with elongated single phase and duplex microstructures", *Ultrasonics*, In press, corrected proof (2012)